

Dartmouth College

Dartmouth Digital Commons

Dartmouth Scholarship

Faculty Work

1995

A Radial Velocity Study of the Dwarf Nova Tz Persei

F. A. Ringwald

Follow this and additional works at: <https://digitalcommons.dartmouth.edu/facoa>

Dartmouth Digital Commons Citation

Ringwald, F. A., "A Radial Velocity Study of the Dwarf Nova Tz Persei" (1995). *Dartmouth Scholarship*. 2510.

<https://digitalcommons.dartmouth.edu/facoa/2510>

This Article is brought to you for free and open access by the Faculty Work at Dartmouth Digital Commons. It has been accepted for inclusion in Dartmouth Scholarship by an authorized administrator of Dartmouth Digital Commons. For more information, please contact dartmouthdigitalcommons@groups.dartmouth.edu.

A radial velocity study of the dwarf nova TZ Persei

F. A. Ringwald^{1,2}★

¹*Department of Physics, Keele University, Keele, Staffordshire ST5 5BG*

²*Department of Physics and Astronomy, Dartmouth College, Hanover, New Hampshire, 03755-3528, USA*

Accepted 1994 November 25. Received 1994 November 22; in original form 1994 October 26

ABSTRACT

A radial velocity study of the H α emission line of the dwarf nova TZ Per is presented. TZ Per has a spectroscopic period of 6.2520 ± 0.0096 h. With this period and published *JHK* photometry, a distance of ≥ 380 pc is inferred. This Z Cam star has both slow outbursts and a short outburst cycle, and time-resolved spectra were obtained on both the rise and the decline of a dwarf nova outburst. TZ Per does not obey the relation between orbital period and outburst decline time found by Bailey and calibrated by Szkody & Mattei. This is probably because the disc is hot all the time, relative to dwarf novae such as U Gem or SS Cyg.

Key words: accretion, accretion discs – binaries: spectroscopic – stars: individual: TZ Per – novae, cataclysmic variables.

1 INTRODUCTION

Dwarf novae are natural laboratories for accretion disc physics. A dwarf nova consists of a K–M dwarf that fills its Roche lobe and spills matter on to a white dwarf, which this red star orbits. The Coriolis acceleration deflects the gas stream, which settles into orbit about the white dwarf. The resulting ring is thought to be broadened into an accretion disc by viscous stress, although the nature of this viscosity is still unclear.

Dwarf novae have quasi-periodic outbursts with amplitudes of 2–5 mag and durations of days to weeks. These outbursts occur in the discs (Warner 1974), and are thought to result from thermal instabilities (Osaki 1974), although mass transfer bursts from the red star may also suffice (Bath 1973). Reviews on dwarf novae, and the cataclysmic variable stars (CVs) of which they are a subclass, include those of Smak (1984), Mattei (1990) and la Dous (1993).

The Z Cam stars are a subclass of dwarf novae, the phenomenology of which was examined by Szkody & Mattei (1984). In addition to normal outbursts, the Z Cam stars have standstills, in which the dwarf nova remains at a brightness of about 1 mag fainter than at outburst maximum for months or even years. Standstills are not completely static, however, since there can appear erratic flareups with amplitudes of several tenths of a magnitude.

Some effort has been made to explain standstills as being a result of enhanced mass flow from irradiation of the red star (Meyer & Meyer-Hofmeister 1983). In this picture, normal outbursts would trigger standstills in CVs with average mass

transfer rates just below the critical rate, above which the disc would be in a steady state (as in the nova-like CVs, which do not have outbursts). The time-scale for these mass transfer rate enhancements is too long, however, of the order of 10^5 yr (Meyer-Hofmeister & Ritter 1993), whereas standstills are observed to last only a few years at most. There is also probably insufficient hard flux to penetrate the atmosphere of the red star (King 1989). It is also unclear observationally whether standstills really are triggered by normal outbursts (see figs 18 and 19 of Lin, Papaloizou & Faulkner 1985, and p. 29 of la Dous 1993). Lin et al. (1985) show that light curves similar to those of Z Cam stars may be reproduced in models that invoke variable mass transfer from the red star, but the cause of this variability is unclear. Standstills are therefore still a mystery.

This paper presents a radial velocity study of the dwarf nova TZ Per, which is a Z Cam star. Bruch & Schimpke (1992) show an optical spectrum, and summarize present knowledge of this object. Coordinates and finding charts are given by Downes & Shara (1993). Bruch, Fischer & Wilmsen (1987) also give a finding chart, although it is incorrect: a corrected chart is given by Bruch, Fischer & Wilmsen (1988).

2 SPECTROSCOPIC OBSERVATIONS

All spectra were taken with the 1.3-m McGraw-Hill telescope, Kitt Peak, Arizona, and its Mark IIIa (black) spectrograph. This all-transmission Cassegrain instrument included a grism with 300 line mm^{-1} , blazed at 26400 \AA and a Hoya Y-50 order-blocking filter. Slit rotation was never used, although atmospheric dispersion effects should be small near

★ Internet: far@astro.keele.ac.uk

$H\alpha$, the line used for the radial velocity study. A slit 2.17 arcsec wide was used for all spectra, and velocity errors were minimized by autoguiding to within 0.2 arcsec.

All spectra covered $\lambda\lambda 6200\text{--}9000\text{ \AA}$ and were taken in two sets during 1991 October. The detector for the spectra taken during October 16–20 UT was the TI-4849 CCD in the BRICC camera (Luppino 1989); the detector for spectra taken October 26 and 27 UT was a geometrically identical Thomson CCD. All nights had 1–2 arcsec seeing, and all nights except October 20 were clear during the observations of TZ Per, although volcanic dust from Mount Pinatubo lit up the sunsets. Table 1 is a journal of the observations.

All spectra had 5 \AA pixel^{-1} dispersion, 11-\AA resolution, and 15-min exposure times. They were debiased, and then flat-fielded with exposures of a tungsten lamp inside the spectrograph. The BRICC spectra were also dark-subtracted. Wavelength calibration used exposures of neon and argon lamps, taken every 30 min between each pair of target spectra. The solutions for the wavelength scales for each night were consistent to within 0.10 \AA , and reproducible to within 0.05 \AA , from the rms residuals of fits to fifth-order polynomials. The spectra were digitally subtracted from the sky spectra that showed through the long slit on both sides of the CCD, and were extracted by simply summing the object columns together, to preserve flux. The spectra were then corrected for atmospheric extinction and flux-calibrated with spectra of the standards HZ44 and G191B2B (Oke

1974), although the extinction seems extreme, redder than $\lambda 8000\text{ \AA}$. Spectra of the hot star HD 19445 (Oke & Gunn 1983) were also taken to map and remove the telluric absorption bands (see Wade & Horne 1988).

3 LIGHT CURVE AND SPECTRUM

Outbursts occur frequently for TZ Per, on average every 17 days, but with wide variation between 4 and 27 days. They typically reach $m_{\text{vis}} = 12.5$; in quiescence, $m_{\text{vis}} = 14.1$ (Szkody & Mattei 1984). A light curve from the AAVSO (Mattei 1992, private communication) is shown in Fig. 1. There is no flat quiescence that intersperses outbursts, as in SS Cyg or U Gem (e.g. Mattei 1990). With the slow rise time documented by Szkody & Mattei (1984), the outburst light curve is roughly a sinusoidal oscillation about a mean. This mean is approximately the brightness of the next standstill, which began two months after this radial velocity study. There was a progressive decrease in outburst amplitude, as well as a progressive brightening of the minimum. Similar behaviour had been noted by Szkody & Mattei (1984) in other Z Cam stars approaching standstill; somehow, a Z Cam star knows it is going to have a standstill well in advance of the event.

For all spectra, velocities (see below) and equivalent widths of the $H\alpha$ emission line were measured, the equivalent widths to within 0.5 \AA . A power law was fitted to each

Table 1. Observations of TZ Per during 1991 October.

HJD ^a	$v(H\alpha)^b$ (km s ⁻¹)	$W(H\alpha)$ (\AA)	α^c	$f_\lambda(6800)^d$	HJD ^a	$v(H\alpha)^b$ (km s ⁻¹)	$W(H\alpha)$ (\AA)	α^c	$f_\lambda(6800)^d$
8545.935	115	3.1	1.98	14.1	8555.828	-1	13.0	1.18	7.1
8545.946	109	2.9	2.10	14.6	8555.839	19	13.2	1.15	6.6
8545.957	61	2.9	2.26	14.4	8555.850	35	13.8	1.05	6.5
8545.968	23	2.9	2.16	14.0	8555.861	67	14.2	1.10	6.2
8546.842	-68	2.5	2.65	35.9	8555.872	71	13.3	1.06	5.9
8546.853	-34	2.5	2.64	37.6	8555.885	118	13.8	0.95	5.8
8546.865	3	2.5	2.80	41.3	8555.895	125	13.7	0.99	5.9
8547.918	-85	4.2	2.78	33.6	8555.907	98	12.8	0.88	5.9
8547.929	-15	3.2	2.75	34.5	8556.602	-33	17.8	1.27	5.6
8548.910	4	3.3	2.63	17.3	8556.613	-27	18.9	1.34	5.7
8548.921	-66	3.9	2.60	17.7	8556.624	15	18.5	1.00	5.7
8549.926	-3	4.1	2.61	7.9	8556.635	45	17.3	1.24	5.4
8549.937	-48	4.2	2.60	10.4	8556.646	62	16.9	1.33	5.5
8555.622	63	12.5	1.10	7.3	8556.657	87	18.6	1.37	5.7
8555.632	97	12.6	1.06	7.2	8556.669	86	17.1	1.17	5.9
8555.644	89	11.7	1.09	7.4	8556.680	119	17.2	1.41	6.1
8555.654	100	11.1	1.29	7.3	8556.691	117	17.3	1.29	6.3
8555.666	82	12.1	1.23	7.4	8556.702	87	16.7	1.18	6.4
8555.677	63	11.8	1.26	7.1	8556.728	49	13.9	1.31	6.4
8555.688	35	12.3	1.25	6.9	8556.738	19	12.4	1.44	6.8
8555.699	-9	10.3	1.37	7.1	8556.849	-73	19.4	1.17	4.7
8555.751	-128	9.9	1.10	6.9	8556.860	-11	19.9	0.76	4.3
8555.762	-147	10.2	1.32	7.4	8556.871	16	17.4	0.95	4.5
8555.784	-104	9.0	1.21	8.1	8556.882	13	19.2	0.87	4.6
8555.795	-90	9.2	1.12	7.7	8556.893	41	18.3	0.88	4.7
8555.806	-70	10.6	1.17	7.7	8556.909	83	19.5	0.20	4.1
8555.817	-46	12.2	1.01	7.5					

^aHeliocentric Julian Date of mid-integration, minus 2 440 000.

^bMeasured with double-Gaussian algorithm, separation 1100 km s^{-1} .

^cIndex of power-law $F_\lambda = k\lambda^{-\alpha}$ fit to continuum, $\lambda\lambda 6350\text{--}6450$ and $6750\text{--}6850\text{ \AA}$.

^dMean flux over $\lambda\lambda 6795\text{--}6805\text{ \AA}$, times $10^{-15}\text{ erg cm}^{-2}\text{ \AA}^{-1}\text{ s}^{-1}$.

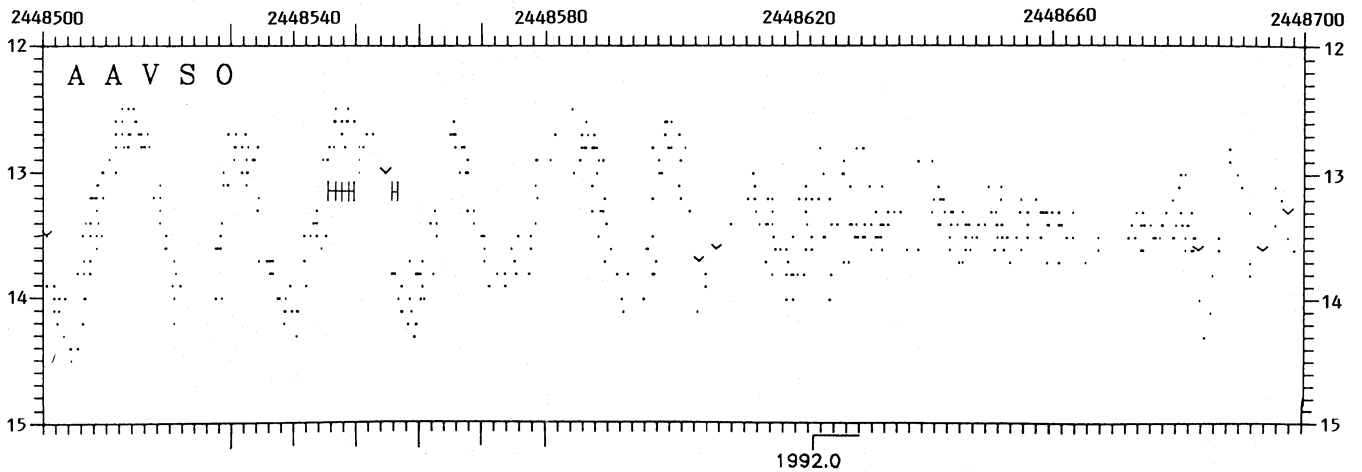


Figure 1. AAVSO light curve, with the nights of spectroscopic observations marked by vertical lines.

spectrum, covering the ranges $\lambda\lambda 6350\text{--}6450\text{ \AA}$ and $\lambda\lambda 6750\text{--}6850\text{ \AA}$, these regions being chosen to avoid the H α and He I lines, and telluric bands. Unfortunately, the entire *R* or *I* bands were not covered by these spectra, but the average flux within $\lambda\lambda 6795\text{--}6805\text{ \AA}$ was measured, to within 5 per cent. These near-monochromatic fluxes showed no obvious periodicities in outburst or in quiescence. All of these measurements were plotted in Figs 2–4, and listed in Table 1.

During quiescence, on October 26 and 27, the individual spectra had average signal-to-noise ratio (S/N) of 27 near H α . Nightly S/N averages are listed in Table 2. The average quiescent spectrum, from October 27, is shown in Fig. 5. No absorption features from the red star were obvious, despite $S/N > 120$. While O I $\lambda 7773\text{ \AA}$ was not detected in the quiescent spectra, even in the nights' average spectra for October 26 and 27, it was in absorption on the rise to outburst (see Fig. 6 and Table 3), as it was in HX Peg (Ringwald 1994). It remained so during outburst maximum and decline (see Fig. 7), as is typical for dwarf novae (Friend et al. 1988). While at maximum and in decline, this line broadened considerably. Although this could have been an effect of the low resolution, it would be of interest to see if this recurs in other outbursts, and in other dwarf novae. The Paschen lines, in emission, were detectable only when TZ Per was in quiescence. Their equivalent widths and those of the He I lines, as well as their widths, are listed in Tables 2 and 3.

4 RADIAL VELOCITY ANALYSIS

The velocities were measured with the algorithm of Schneider & Young (1980), in which the spectral line to be measured is convolved with a positive and a negative Gaussian of settable width and separation, with the zero of this convolution taken as the velocity. Gaussians of width 640 km s^{-1} (slightly larger than one resolution element) were used, to avoid jitter from noise variations. After trying separations – between the positive Gaussian and the negative Gaussian – ranging from 640 to 1710 km s^{-1} , a separation of 1100 km s^{-1} was found to maximize K_{em}/σ in the sinusoidal fit below. While this method is often used in measuring the velocities of CV emission lines, since it concentrates on

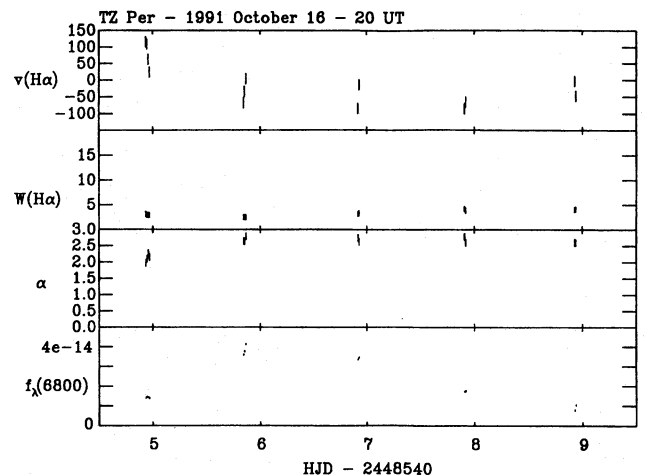


Figure 2. Radial velocity of H α (top), equivalent width of H α (middle-top), index α of power-law $F_{\lambda} = k\lambda^{-\alpha}$ fitted to $\lambda\lambda 6350\text{--}6450\text{ \AA}$ and $\lambda\lambda 6750\text{--}6850\text{ \AA}$ (middle-bottom), and average flux (f_{λ}) within $\lambda\lambda 6795\text{--}6805\text{ \AA}$, in units of $\text{erg cm}^{-2}\text{ \AA}^{-1}\text{ s}^{-1}$ (bottom), for 1991 October 16–20 UT.

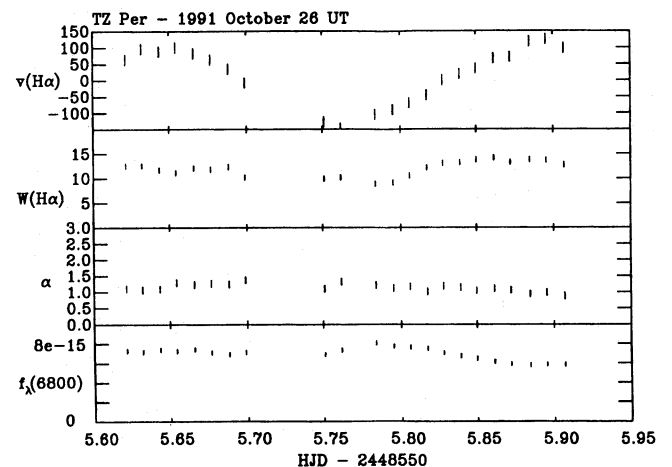


Figure 3. Same as Fig. 2, but for 1991 October 26 UT.

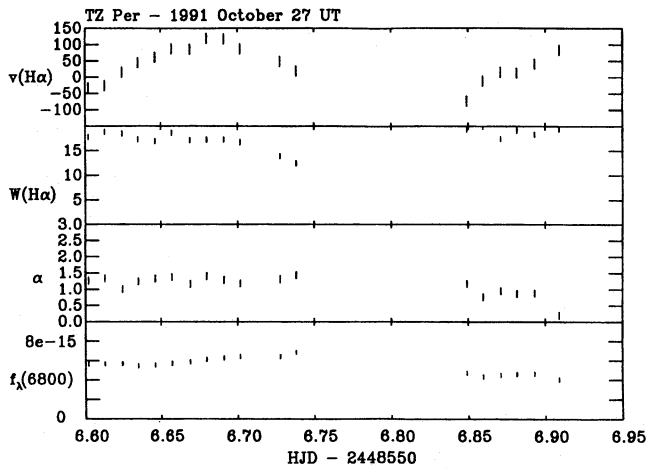


Figure 4. Same as Fig. 2, but for 1991 October 27 UT.

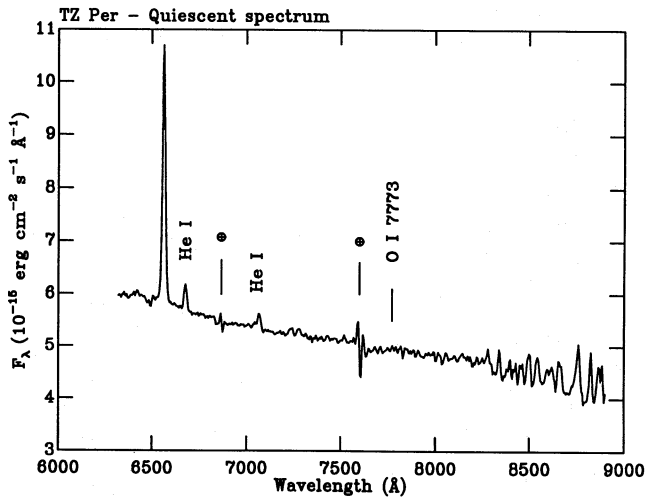


Figure 5. Average of all spectra from 1991 October 27 UT, while in quiescence, of 4.5-h total exposure time over 7.4 h. Wrinkles in the spectrum caused by imperfect telluric band removals are marked by ⊕.

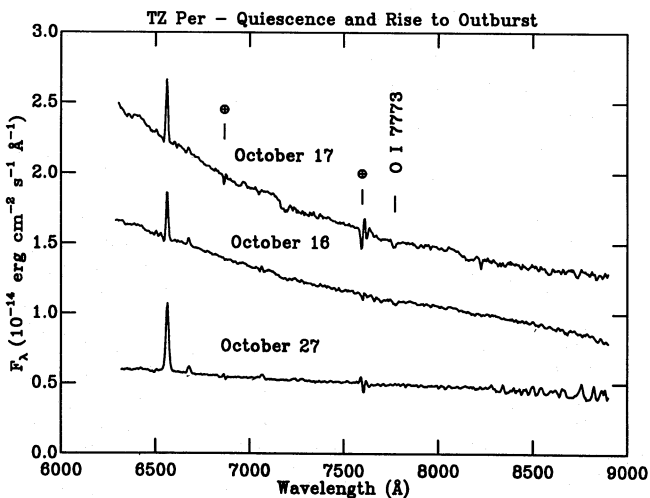


Figure 6. Spectra of quiescence and rise to outburst. Each spectrum represents the average of all spectra taken that night.

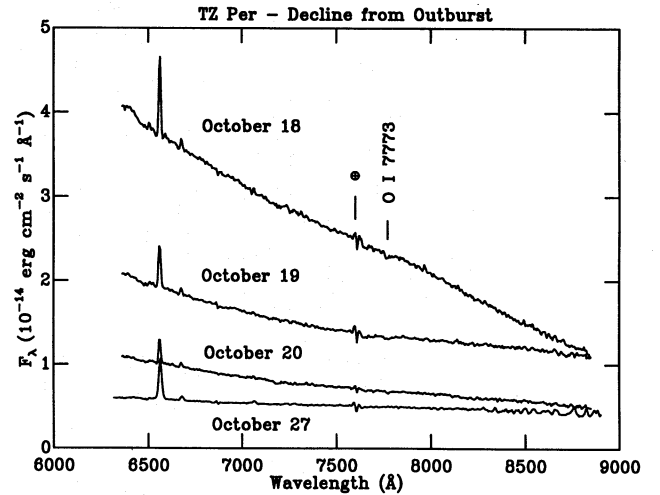


Figure 7. Spectra of decline from outburst. Each spectrum represents the average of all spectra taken that night.

Table 2. Emission lines in summed spectra.

	Hα	He I	He I	O I	Pa14	CaII	Pa12	Pa11
	6563	6678	7065	7773	8598	8662	8750	8862
October 26 – quiescent								
S/N = 130								
W(Å)	11.7	1.3	0.9	> -0.1	1.4	1.8	3.5	1.6
FWHM (km s⁻¹)	900	700	800	-	1150	1000	950	1250
October 27 – quiescent								
S/N = 110								
W(Å)	17.0	1.5	1.4	> -0.1	4.0	3.5	6.0	3.5
FWHM (km s⁻¹)	850	700	800	-	1600	800	900	1000

Table 3. Emission lines in summed spectra.

	Hα	He I	He I	O I
	6563	6678	7065	7773
October 16 – rise				
S/N = 150				
W(Å)	2.9	0.5	0.3	-1.0
FWHM (km s⁻¹)	500	400	400	850
October 17 – rise				
S/N = 160				
W(Å)	2.5	0.4	-	-0.6
FWHM (km s⁻¹)	650	450	-	700
October 18 – maximum				
S/N = 125				
W(Å)	3.3	0.5	-	-0.9
FWHM (km s⁻¹)	600	450	-	1100
October 19 – decline				
S/N = 90				
W(Å)	4.3	0.6	0.2	-0.8
FWHM (km s⁻¹)	800	600	650	1600
October 20 – decline				
S/N = 65				
W(Å)	4.4	0.8	0.4	-0.7
FWHM (km s⁻¹)	700	600	600	900

the gross motion of the line and avoids the poorly understood low-velocity motions in the line core, it is not clear that it reflects the dynamics of the white dwarf any better, since the emission line arises in the disc, which is not necessarily symmetrically distributed around the white dwarf (e.g. Marsh, Horne & Shipman 1987). All velocities were heliocentrically corrected, and all times were rewritten as heliocentric times of mid-integration.

A Lomb-Scargle periodogram (Press et al. 1992) was computed (see Fig. 8) from these velocities, which shows a strong periodicity at 0.2605 d. The velocities were then fitted by least squares to

$$V(t) = \gamma_{\text{em}} + K_{\text{em}} \sin[2\pi(t - T_0)/P_{\text{orb}}],$$

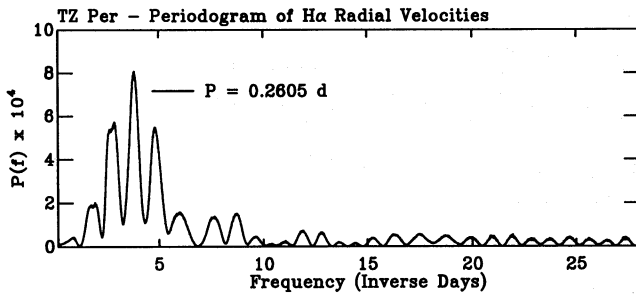


Figure 8. Periodogram of H α velocities, using Lomb-Scargle method (Press et al. 1992).

with the resulting parameters listed in Table 4 (see also Fig. 9). All errors were to 68 per cent confidence, computed with the likelihood ratio test of Cash (1979); errors on individual velocities were estimated at 10–15 km s⁻¹, from measurements of the O I λ 6300-Å night sky line. The Monte Carlo analysis of Thorstensen & Freed (1985) gave a correctness likelihood for the alias choice and a discriminatory power for the time series to make the distinction that were both well in excess of 99 per cent; thus the alias choice is secure.

5 DISCUSSION

The orbital period found was 6.2520 ± 0.0096 h. This does not agree with the linear relation between orbital period and outburst decline duration found by Bailey (1975) and refined by Szkody & Mattei (1984), which predicted a period of 3.70 h. All other orbital periods predicted with this relation by Szkody & Mattei agreed within 10 per cent of the measured orbital periods (see Table 5). This so-far purely empirical relation may be linking the amount of heat in a disc, which leaks out of the disc at a certain rate, with its size, which is a function of orbital period since it is bounded by the Roche lobe. Since this disc seems to oscillate around a mean near the standstill state and not to decline to and stay at a minimum, it should be relatively hot all the time, never cooling as much as the discs in dwarf novae such as SS Cyg

Table 4. TZ Per – derived orbital parameters.

	P_{orb} (days)	K_{em} (km s ⁻¹)	γ_{em} (km s ⁻¹)	T_0 (HJD – 2440000)	σ (km s ⁻¹)
Quiescent (26 & 27)	0.2605 ± 0.0004	112 ± 3	-6 ± 2	8555.832 ± 0.001	15

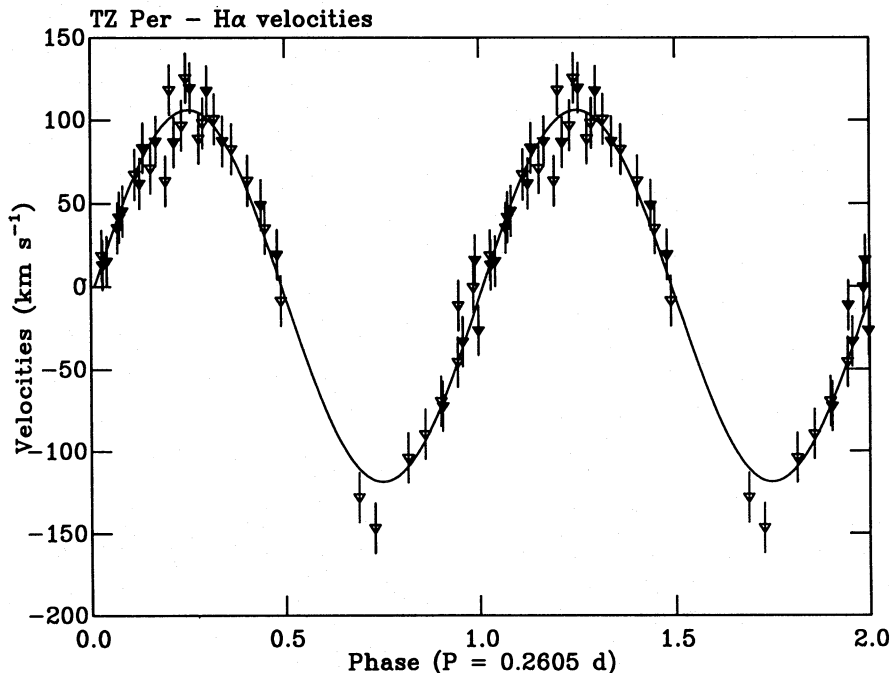


Figure 9. Least-squares fit of H α velocities from October 26 and 27 to a sinusoid of period 0.2605 d. Open triangles represent velocities from October 26; closed triangles, from October 27.

Table 5. Predicted versus measured orbital periods.

	Predicted ^a	Measured	References
AR And	2.03	2.25 ± 0.25	Szkody 1985
X Leo	3.70	3.946 ± 0.002	Shafter & Harkness 1986
CZ Ori	5.37	5.254 ± 0.005	Ringwald, Thorstensen & Hamwey 1994
KT Per	3.70	3.92 ± 0.03	Ratering, Bruch & Diaz 1993
TZ Per	3.70	6.252 ± 0.010	this work

^aPredicted by Szkody & Mattei (1984), from the relation between orbital period and time of decline from outburst (see Bailey 1975).

or U Gem. One might therefore have expected such a hot disc to take less time to decline, and such a short decline time would have led us to predict too short an orbital period.

Two other relations from Szkody & Mattei (1984), between orbital period and both total outburst time and rise time, predict an orbital period of 6.03 h. This is closer to the observed period than is the prediction from the relationship involving decline time. It is not clear whether these two relations are valid for the other dwarf novae, however, since only in one case (the total outburst time for X Leo) do they predict an orbital period to within 10 per cent.

With the orbital period and *JHK* photometry, the distance to TZ Per was estimated. First, the radius of the red star was estimated by

$$R/R_{\odot} = 3.04 \times 10^{-5} P_{\text{orb}}(\text{s})$$

(Warner 1976), so that here, $R = 0.68 R_{\odot}$. The spectral type of the red star was then estimated by comparison with the plot of *M* dwarf radius versus spectral type of Mateo, Szkody & Bolte (1985); a small extrapolation gave K7–M0.

The fraction of infrared light in the *K*-band attributable to the red star was found next. Using the flux ratios between the *J*, *H* and *K* bands, and the lever-arm technique of Berriman, Szkody & Capps (1985), I found 52 per cent and 44 per cent, respectively, for the magnitudes of Szkody (1977) ($J = 12.11$, $H = 11.96$ and $K = 11.81$) and Sherrington & Jameson (1983) ($J = 11.78$, $H = 11.54$ and $K = 11.23$). The red star in TZ Per would therefore have either $K_2 = 12.52$ or $K_2 = 12.12$. The near-constancy of *K*-band surface brightness (S_k) with radius in lower main-sequence stars was then used to calculate

$$5 \log d = K_2 - S_k + 5 + 5 \log(R/R_{\odot})$$

(Bailey 1981), using $3.787 < S_k < 3.895$ from the recalibration of Ramseier (1994), for a K7–M0 dwarf, which should have $3.16 < V - K < 3.65$ (Bessell & Brett 1988).

The distance is therefore 361–380 or 301–316 pc, for the *JHK* magnitudes of Szkody (1977) and Sherrington & Jameson (1983), respectively. This result should be regarded as a lower limit, since both sets of *JHK* magnitudes were made when TZ Per was in standstill, so the accretion disc was probably optically thick and its contribution may be underestimated. The distance that should be adopted is therefore ≥ 380 pc.

For the apparent magnitude in standstill of $m_{\text{vis}} = 13.4$ (see Fig. 1), this means $M_v \leq 5.5$. If the red star were a K7–M0 dwarf, it should be present in the visual at a dilution of about 5–8 per cent. Its absorption features were probably not

detected because they should be weak at this spectral type (see fig. 3 of Wade & Horne 1988), although with higher spectral resolution and comparable S/N, they might be.

ACKNOWLEDGMENTS

The author held a Dartmouth Fellowship when the spectra were taken, and now holds a PPARC/SERC Postdoctoral Research Fellowship. The spectroscopic observations were made at the Michigan–Dartmouth–MIT Observatory, which is owned and operated by a consortium of the University of Michigan, Dartmouth College, and the Massachusetts Institute of Technology. I thank Dr John Thorstensen, who wrote much of the analysis software; some analysis was done with the ARK software on the Keele STARLINK node. The AAVSO Director, Dr Janet A. Mattei, sent data from the international AAVSO data base, and I thank all the observers who contributed, especially Dave York, who specially monitored this star and called up nightly with his visual magnitudes. I also thank the referee, Dr Robert Smith, for helpful suggestions.

REFERENCES

- Bailey J., 1975, *J. Br. Astron. Assoc.*, 86, 30
- Bailey J., 1981, *MNRAS*, 197, 31
- Bath G. T., 1973, *Nat. Phys. Sci.*, 246, 84
- Berriman G., Szkody P., Capps R. W., 1985, *MNRAS*, 217, 327
- Bessell M. S., Brett J. M., 1988, *PASP*, 100, 1134
- Bruch A., Schimpke T., 1992, *A&AS*, 93, 419
- Bruch A., Fischer F.-J., Wilmsen U., 1987, *A&AS*, 70, 481
- Bruch A., Fischer F.-J., Wilmsen U., 1988, *A&AS*, 74, 351
- Cash W., 1979, *ApJ*, 228, 939
- Downes R. A., Shara M. M., 1993, *PASP*, 105, 127
- Friend M. T., Martin J. S., Smith R. C., Jones D. H. P., 1988, *MNRAS*, 233, 451
- King A. R., 1989, *MNRAS*, 241, 365
- la Dous C., 1993, in Hack M., la Dous C., eds, *Cataclysmic Variables and Related Objects*. NASA/CNRS Monograph Series on Non-Thermal Phenomena in Stellar Atmospheres, NASA, p. 15
- Lin D. N. C., Papaloizou J., Faulkner J., 1985, *MNRAS*, 212, 105
- Luppino G. A., 1989, *PASP*, 101, 931
- Marsh T. R., Horne K., Shipman H. L., 1987, *MNRAS*, 225, 551
- Mateo M., Szkody P., Bolte M., 1985, *PASP*, 97, 45
- Mattei J. A., 1990, in İbanoğlu C., ed., *Active Close Binaries*. Kluwer, Dordrecht, p. 611
- Meyer F., Meyer-Hofmeister E., 1983, *A&A*, 121, 29

- Meyer-Hofmeister E., Ritter H., 1993, in Sahade J., McCluskey G., Kondo Y., eds, *The Realm of Interacting Binary Stars*. Kluwer, Dordrecht, p. 143
- Oke J. B., 1974, *ApJS*, 27, 21
- Oke J. B., Gunn J. E., 1983, *ApJ*, 266, 713
- Osaki Y., 1974, *PASJ*, 26, 429
- Press W. H., Teukolsky S. A., Vetterling W. T., Flannery B., 1992, *Numerical Recipes in C*, Second Edition. Cambridge Univ. Press, Cambridge, p. 575
- Ramseyer T. F., 1994, *ApJ*, 425, 243
- Ratering C., Bruch A., Diaz M., 1993, *A&A*, 268, 694
- Ringwald F. A., 1994, *MNRAS*, 270, 804
- Ringwald F. A., Thorstensen J. R., Hamwey R. M., 1994, *MNRAS*, 271, 323
- Schneider D. P., Young P. J., 1980, *ApJ*, 238, 946
- Shafter A. W., Harkness R. P., 1986, *AJ*, 92, 658
- Sherrington M. R., Jameson R. F., 1983, *MNRAS*, 205, 265
- Smak J., 1984, *PASP*, 96, 5
- Szkody P., 1977, *ApJ*, 217, 140
- Szkody P., 1985, *AJ*, 90, 1837
- Szkody P., Mattei J. A., 1984, *PASP*, 96, 988
- Thorstensen J. R., Freed I. W., 1985, *AJ*, 90, 2082
- Wade R. A., Horne K., 1988, *ApJ*, 324, 411
- Warner B., 1974, *Mon. Notes Astron. Soc. S. Afr.*, 33, 21
- Warner B., 1976, in Eggleton P., Mitton S., Whelan J., eds, *Structure and Evolution of Close Binary Systems*. Reidel, Boston, p. 85